VALENCE XPS STRUCTURE AND CHEMICAL BOND IN $Cs_2UO_2Cl_4$

by

Yury A. TETERIN [1,2*], ***Konstantin I. MASLAKOV*** [2], ***Mikhail V. RYZHKOV*** [3], ***Anton Yu. TETERIN*** [1], ***Kirill E. IVANOV*** [1], ***Stepan N. KALMYKOV*** [2], ***Vladimir G. PETROV*** [2], ***and Dmitry N. SUGLOBOV*** [4]

[1]NRC "Kurchatov Institute", Moscow, Russia
[2] Chemistry Department, Lomonosov Moscow State University, Moscow, Russia
[3] Institute of Solid State Chemistry, Ural Department of RAS, Ekaterinburg, Russia
[4] V.G. Khlopin Radium Institute, St.-Petersburg, Russia

Scientific paper
DOI: 10.2298/NTRP1601037T

Quantitative analysis was done of the valence electrons X-ray photoelectron spectra structure in the binding energy (BE) range of 0 eV to ~35 eV for crystalline dicaesium tetrachloro-dioxouranium (VI) ($Cs_2UO_2Cl_4$). This compound contains the uranyl group UO_2^{2+}. The BE and structure of the core electronic shells (~35 eV-1250 eV), as well as the relativistic discrete variation calculation results for the $UO_2Cl_4^{2-}$ (D_{4h}) cluster reflecting U close environment in $Cs_2UO_2Cl_4$ were taken into account. The experimental data show that many-body effects due to the presence of cesium and chlorine contribute to the outer valence (0-~15 eV BE) spectral structure much less than to the inner valence (~15 eV-~35 eV BE) one. The filled U5f electronic states were theoretically calculated and experimentally confirmed to be present in the valence band of $Cs_2UO_2Cl_4$. It corroborates the suggestion on the direct participation of the U5f electrons in the chemical bond. Electrons of the U6p atomic orbitals participate in formation of both the inner (IVMO) and the outer (OVMO) valence molecular orbitals (bands). The filled U6p and the O2s, Cl3s electronic shells were found to make the largest contributions to the IVMO formation. The molecular orbitals composition and the sequence order in the binding energy range 0 eV-~35 eV in the $UO_2Cl_4^{2-}$ cluster were established. The experimental and theoretical data allowed a quantitative molecular orbitals scheme for the $UO_2Cl_4^{2-}$ cluster in the BE range 0-~35 eV, which is fundamental for both understanding the chemical bond nature in $Cs_2UO_2Cl_4$ and the interpretation of other X-ray spectra of $Cs_2UO_2Cl_4$. The contributions to the chemical binding for the $UO_2Cl_4^{2-}$ cluster were evaluated to be: the OVMO contribution – 76%, and the IVMO contribution – 24 %.

Key words: actinide, uranium, electronic structure, XPS, relativistic calculation

INTRODUCTION

Uranium compounds are important in atomic industry all the way from nuclear fuel production to radioactive waste management and disposal, as well as solution of ecological problems of environment rehabilitation. Therefore, electronic structure and chemical bond nature in uranium, in particular uranyl, compounds, is a topic of a great interest [1-5]. The XPS method is used in studies of uranyl compounds also [6]. These compounds contain an almost linear group UO_2^{2+} [6]. The valence XPS of U(IV) compounds exhibit a sharp peak attributed to the quasi atomic U5f electrons around zero binding energy (BE) [7-9]. This peak is absent in the XPS of U(VI) compounds [1-3]. In the $U6p_{3/2}$ BE range the XPS of uranyl compounds instead of a sharp single peak exhibit the two explicit, several eV distant from each other, peaks [1-4]. Peaks in the valence band are several eV wide, which is sometimes wider than the corresponding core electron peaks [5, 6]. For example, the O1s peak (E_b = 531.6 eV) full width at half maximum (FWHM) (Γ, eV) for $Cs_2UO_2Cl_4$ is Γ = = 1.6 eV, while the corresponding O2s (E_b~24.5 eV) peak is ~4 eV wide and structured. It contradicts the Heisenberg uncertainty ratio $\Delta E \Delta \tau \quad h/2$, where ΔE is the natural width of a level from which an electron was extracted, τ – the hole life-time, and h – the Planck constant. Since the hole lifetime (τ) grows as the absolute atomic level energy decreases, the lower BE XPS atomic peaks are expected to be narrower. For $Cs_2UO_2Cl_4$ [5] and UO_2X_2 (X = Br, Cl, F) [4] it is *vice versa*. It shows that the peaks observed in the 0 - ~ 35 eV BE range are not purely atomic. This fact stimulated experimental and theoretical studies of the low BE XPS

* Corresponding author; e-mail: teterin_YA@nrcki.ru

structure in compounds of actinides [6], lanthanides [10] and other elements [5]. One of the reasons for such an XPS structure formation was established to be the outer (OVMO; 0-~15 eV BE) and the inner (IVMO; ~15-~35 eV BE) valence molecular orbitals formation, with significant participation of the An6p and the O2s filled atomic shells [5, 6]. Practically, these spectra reflect the valence band (0 eV-~35 eV BE) structure. They are observed as bands several eV wide. These data agree qualitatively and some quantitatively, with theoretical non-relativistic [3, 4] and relativistic [11-14] calculation results.

A special attention has been paid to the study of the uranyl group, whose electronic structure was considered in the non-relativistic approximation in [15-17]. Position of Cs^+ ions regarding to the uranyl group containing clusters for some of the U(VI) compounds and the correlation of the U4f – O1s BE difference with the $R_{U\text{-}O}$ interatomic distance, are given in [18]. The participation of the U6p and the O2s electrons in the U-O binding in uranyl group was considered in [19-22]. Despite the fact that correlation of the OVMO- and IVMO- related structure parameters with physical and chemical properties of uranium compounds have been thoroughly studied, the role of the U6p electrons in the chemical bond is still not clear.

The XPS study of oxidation states and chemical bond nature in compounds [5], including those of lanthanides [10] and actinides [6], beside peak intensities (I_o) and chemical shifts (E_b), employs BE differences between core and valence levels (E_i) and spectral structure parameters. The XPS structure can result from the OVMO and IVMO formation, spin-orbit splitting (E_{sl}), multiplet splitting (E_{ms}), induced charge (E_{ind}), many-body perturbation (E_{sat}), dynamic effect (gigantic Coster-Kronig transitions), Auger process, *etc*. [5, 6, 10].

Several mechanisms of the structure formation, exhibited simultaneously with similar probability, do not allow a correct interpretation of the XPS spectra. If one of the structure formation mechanisms prevails, parameters of such a structure correlate quantitatively with physical and chemical properties of the studied compound. These structure parameters provide information on: degree of delocalization and participation of electrons in chemical binding; electronic configuration and oxidation states of An(N) ions; density of the uncoupled An5f electrons on paramagnetic ions; degree of participation of filled electronic shells of metals and ligands in the OVMO and IVMO formation, structure and nature of the molecular orbitals (MO); local environment structure, *etc*. [7-9, 14, 23-26].

The 0-~35 eV BE XPS range is especially important since it reflects the MO structure and with the photoionization cross-sections in mind, reflects the total valence density of occupied states. However, this BE range XPS interpretation requires understanding of how effective (experimentally observable) structure formation mechanisms manifest. Therefore, the core (~35-1250 eV BE) XPS structure has to be studied in order to evaluate the contributions of certain structure formation mechanism to the valence band XPS [5, 6, 10].

The quantitative interpretation of the valence XPS structure of uranyl compounds, taking into account the photoelectron, conversion, emission and other X-ray spectral data and relativistic calculation results, was done for γ-UO_3 [14, 27] and UO_2F_2 [26].

The present work quantitatively interpreted the valence XPS structure of $Cs_2UO_2Cl_4$ single crystal in the BE range 0-~35 eV. In order to understand the chemical bond nature and to evaluate the contributions of the OVMO and the IVMO electrons to this bond, the binding energies, core-valence BE differences, core electron spectral structure parameters (~35-1250 eV BE), as well as the relativistic, self-consisting field discrete variation (SCF RDV) calculation results for the $UO_2Cl_4^{2-}(D_{4h})$ cluster, reflecting U close environment in $Cs_2UO_2Cl_4$.

EXPERIMENTAL

Samples

Crystalline double cesium uranyl chloride $Cs_2UO_2Cl_4$ was prepared the same way as in [28] by adding of the stoichiometric quantity of cesium chloride to uranyl acetate solved in weak hydrochloric acid, followed by re-crystallization. For the XPS study, the ~7 3×1 mm^3 $Cs_2UO_2Cl_4$ crystal was glued with conductive glue to a metallic substrate. During the XPS measurements, the sample surface was cleaned mechanically with a scraper. The CsCl sample was prepared as a tablet from finely dispersed powder pressed in In on Ti substrate.

X-ray photoelectron measurements

XPS spectra were measured with an electrostatic spectrometer HP 5059A using AlK $_{1,2}$ ($h\nu$ = 1486.6 eV) radiation under 1.3 10^{-7} Pa at room temperature. The low-energy electrons gun was used for the compensation of sample charging during the photo emission. The device resolution measured as the full width on at the half-maximum (FWHM) of the AU4f$_{7/2}$ peak was 0.7 eV. The binding energies E_b(eV) were measured relatively to the BE of the C1s electrons from hydrocarbons absorbed on the sample surface that was accepted to be equal to 285.0 eV. The error in the determination of the BE and the peak widths did not exceed 0.1 eV, that of the relative peak intensity – 10 %. The FWHM are given relatively to that of the C1s XPS peak from hydrocarbon on the sample surface, being 1.3 eV. The background due to the inelastically scat-

tered electrons was subtracted by the Shirley method [29].

The valence and the core electron XPS structure for the studied sample in the BE range 0 eV-1250 eV is typical for $Cs_2UO_2Cl_4$. It confirms unambiguously the presence of $Cs_2UO_2Cl_4$ on the substrate surface [30]. The studied samples were proven not to contain more than 0.5 weight % of impurities, since foreign peaks were not observed in the whole XPS BE range 0 eV-1250 eV.

The quantitative elemental analysis of several nanometer-deep layers, of the studied samples, was done. It was based on the fact that the spectral intensity is proportional to the number of certain atoms in the studied sample. The following ratio was used: $n_i/n_j = (S_i/S_j)(k_j/k_i)$, where n_i/n_j is the relative concentration of the studied atoms, S_i/S_j – the relative core-shell spectral intensity, and k_j/k_i – the relative experimental sensitivity coefficient. The following coefficients were used: 1.00 (C1s), 2.80 (O1s), 2.92 (Cl2p), 1.48 (Cl 2s and, 36.00 ($U4f_{7/2}$) (see *e. g.* [31]). The stoichiometric composition was satisfactory for $Cs_2UO_2Cl_4$.

CALCULATIONS

In $Cs_2UO_2Cl_4$ uranium is surrounded by two oxygen ions in the axial directions (uranyl group UO_2^{2+}) and by four chlorine ions in the equatorial plane. The crystal structure parameters are: $R_{U\text{-}O} = 0.1774(4)$ nm and $R_{U\text{-}Cl} = 0.2671(1)$ nm [32]. As it is expected, these parameters are comparable to those of $Cs_2NpO_2Cl_4$: $R_{Np\text{-}O} = 0.1758(2)$ nm, $R_{Np\text{-}Cl} = 0.2657(5)$ nm [16], and $Cs_2PuO_2Cl_4$: $R_{Pu\text{-}O} = 0.1752(3)$ nm and $R_{Pu\text{-}Cl} = 0.26648(8)$ nm [33]. In order to evaluate the influence of interatomic distances on the MO energies in the Cl3s BE range,the electronic structure calculations were done for the three clusters of $UO_2Cl_4^{2-}$ with interatomic distances: (a) $R_{U\text{-}O} = 0.171$ nm and $R_{U\text{-}Cl} = 0.262$ nm; (b) $R_{U\text{-}O} = 0.174$ nm and $R_{U\text{-}Cl} = 0.264$ nm; (c) $R_{U\text{-}O} = 0.1772$ nm and $R_{U\text{-}Cl} = 0.2671$ nm (equilibrium position). To evaluate the orbital forces, the calculations were done for: (a) $R_{U\text{-}O} = 0.1772$ nm and $R_{U\text{-}Cl} = 0.2671$ nm; (b) $R_{U\text{-}O} = 0.1792$ nm, and $R_{U\text{-}Cl} = 0.2671$ nm; (c) $R_{U\text{-}O} = 0.1772$ nm and $R_{U\text{-}Cl} = 0.2691$.

For the case of the $UO_2Cl_4^{2-}$ cluster, the re-normalization of the valence oxygen and chlorine atomic orbital (AO) populations during the self-consistency, was done. The latter model of small cluster boundary condition also allows one to include into the iterative scheme the stoichiometry of the compound and the possibility of charge redistribution between the outer atoms in the cluster and the surrounding crystal.

In the present paper, the electronic structure is calculated in the density functional theory (DFT) approximation using the original code of the fully relativistic discrete variation (RDV) cluster method [34, 35], with exchange-correlation potential [36]. The RDV method is based on the solution of the Dirac-Slater equation for 4-component wave functions transforming according to the irreducible representations of the double point group (D_{4h} in the present calculations). For the calculation of symmetry coefficients, we used the original code, which realizes the projection operators technique [34] and includes the matrices of the irreducible representations of double point groups [37] and the transformation matrices presented in [38]. The extended basis of the 4-component numerical atomic orbitals, obtained as the solution of the Dirac-Slater equation for the isolated neutral atoms, also included the $U7p_{1/2}$ and the $U7p_{3/2}$ functions in addition to the occupied AO. The use of such "most natural basis orbitals" and the absence of any muffin-tin (M-T) approximation to potential and electronic density, allow one to describe the formation of inter-atomic bonds. In such an approach, this description is more illustrative than that obtained in the band structure approach. Numerical Diophantine integration in matrix elements calculations was carried out for 22000 ($UO_2Cl_4^{2-}$) points distributed in the cluster space. It provided the convergence of MO energies better than 0.1 eV.

RESULTS AND DISCUSSION

As mentioned previously, the valence (0-~35 eV BE) XPS structure of $Cs_2UO_2Cl_4$ must reflect the MO structure. In order to evaluate the contribution of other mechanisms to the valence XPS formation, the core electron XPS structure of $Cs_2UO_2Cl_4$, was analyzed.

Core-electron XPS structure of $Cs_2UO_2Cl_4$

Electron BE in the 0-1250 eV range for $Cs_2UO_2Cl_4$ are given in tab. 1. The data for UO_2F_2 [26], metallic U [39, 40] and calculation results for atomic U [41], as well as photo-ionization cross-sections [42, 43] are given for comparison. The data for CsCl are given in square brackets (tab. 1) at the end of the column for UO_2F_2. The basic peaks of CsCl XPS in the BE range 0-1250 eV are intense and contain the many-body perturbation-related structure at the higher BE side. This structure makes the identification of uranium peaks in the $Cs_2UO_2Cl_4$ XPS difficult. Therefore, the valence and core XPS structure of CsCl was studied carefully in the BE range 0-1250 eV. For example, the Cs3d XPS ($E_b(Cs3d_{5/2}) = 724.5$ eV) exhibits the 20 % and 50 % intensity regarding to the basic peaks satellites 11.8 eV and 23.6 eV away from the basic peaks, respectively. The Cl2p XPS ($E_b(Cl2p_{3/2}) = 198.7$ eV) exhibits such satellites which are 8 % and 25 % intense, 10.0 eV and 19.0 eV away from the basic peaks, respectively [6]. Since intensity of such satellite is known to drop as the BE decreases [10], the

Table 1. Electron binding energies E_b [eV] and photoionization cross-sections σ[a] at 1486.6 eV

U*nlj* O*nlj*	$Cs_2UO_2Cl_4$	UO_2F_2[b]	UO_2[c]	U[d]	U_{Theor}[e]	σ
U5f	–	–	1.9 (1.5)	0.5 (2.0)	0.5	22.0
$U6p_{3/2}$	15.4 19.8(3.1)[f]	15.6(3.5) 20.1(3.5)	18.0(3.1)	16.8	18.3	5.14
$U6p_{1/2}$	30.9		28.5(3.5)	26.8	28.3	1.78
U6s	48.2(7.0)	49.3(6.0)	47.0(6.0)	43.9	49.3	2.28
$U5d_{5/2}$	98.1(2.3)	99.2(2.2)	97.3(2.5)	94.2	96.3	47.0
$U5d_{3/2}$	106.9(2.7)	107.9(2.7)	105.5(3.9)	102.8	107.6	32.1
$U5p_{3/2}$	–	197.7 200.2	197.4(7.8)	194.8	205.9	30.2
$U5p_{1/2}$	–	264.1(7.0)	–	258.4	261.1	9.16
U5s	–	–	–	~323.7	327.9	10.0
$U4f_{7/2}$	382.1(1.6)	383.4(2.1)	380.9(2.1)	377.4	379.3	372
$U4f_{5/2}$	393.0(1.6)	394.1(2.1)	391.8(2.1)	388.2	390.7	291
$U4d_{5/2}$	740.6	741.5(4.7)	739.3(5.9)	736.2	741.9	233
$U4d_{3/2}$	783.1(4.7)	784.0(4.7)	781.6 (6.0)	778.3	784.5	153
$U4_{p3/2}$	1044.9(7.3)	1048.2(7.8)	1046.7(7.4)	1043.0	1050.6	106
O2p	~5.6(2.9)	~6.1(4.2)	~6.1(5.0)			0.27
O2s	~24.5	25.0(3.5)	23.3 24.8			1.91
O1s	531.6(1.6)	532.4(1.8)	530.5(1.6)			40.0
Cs6s						0.16
$Cs5p_{3/2}$	10.4(1.4)	[10.1(1.2)][g]				4.52
$Cs5p_{1/2}$	12.0	11.7				2.31
Cs5s	23.8(2.0)	[23.4(1.4)]				2.50
Cl3p		[4.4(1.4)]				2.35
Cl3s	16.0(2.3)	[15.0(1.2)]				2.52
$Cl2p_{3/2}$	198.7(1.2)	[198.6(1.2)]				20.6

[a] Photo-ionization cross-sections σ (kilo barn (10^{-25} m^2) per atom) from [42]; [b]Values for UO_2F_2 from [26]. E_b(F2s) = 29.9 eV and E_b(F1s) = 685.3 eV; [c] Values for UO_2 from [27]; [d] Values for metallic U from [39, 40]; [e] Calculation data from [41], Values given relative to the U5f peak from metallic U; [f] FWHM relative to Γ(C1s) = 1.3 eV are given in parentheses; [g] Values on CsCl are given in brackets

satellites in the valence XPS are expected to be the least intense. The Cs and Cl XPS structure, as well as the satellite structure, complicate significantly the interpretation of $Cs_2UO_2Cl_4$ XPS in the 0-1250 eV BE range.

The O1s XPS of $Cs_2UO_2Cl_4$ was observed as a widened single peak at E_b(O1s) = 531.6 eV and FWHM Γ(O1s) = 1.6 eV (fig. 1). The U4f XPS from $Cs_2UO_2Cl_4$, at the highest probability, shows the many-body perturbation-related structure attributable to an extra electronic transition within the filled and the vacant valence levels during the U4f photo emission (fig. 2). It appears as shake-up satellites, whose parameters reflect the MO structure. As a result, the U4f XPS consists of the spin-orbit split doublet with E_{sl}(U4f) = 10.9 eV, and the shake-up satellites at the

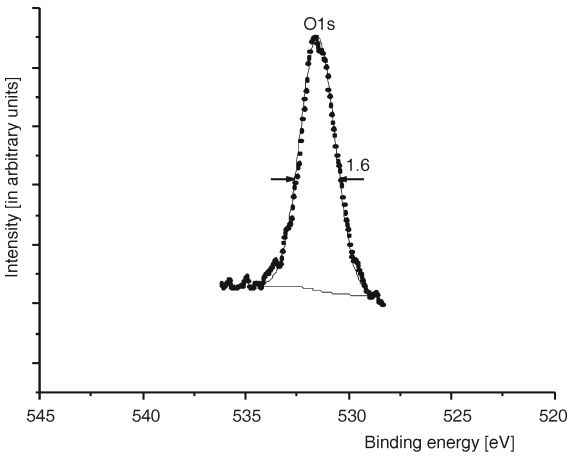

Figure 1. O1s XPS from $Cs_2UO_2Cl_4$

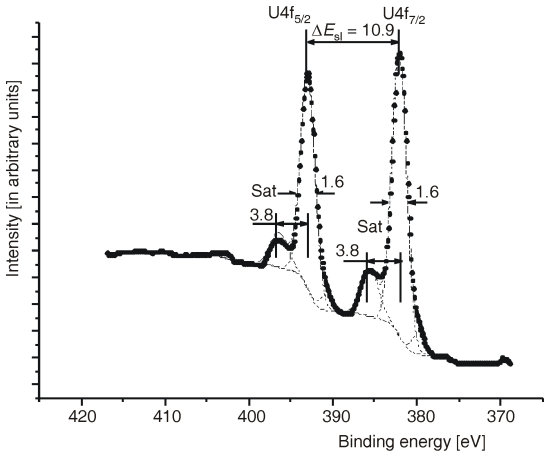

Figure 2. U4f XPS from $Cs_2UO_2Cl_4$

higher BE side with E_{sat} = 3.8 eV. The satellite intensity ($I_{sat} = I_s/I_o$) calculated as the ratio of the XPS satellite area (I_s) to the basic peak area (I_o) was 19 %. Such structure parameters can determine the actinide ion oxidation state as An(VI). The U4f XPS structure is typical for actinide oxidation state An(VI): U(VI) [9, 14, 24, 26], Np(VI) and Pu(VI) [6]. The shake-up satellites are known to appear in the XPS of any core levels of uranium compounds, and the satellite intensity decreases as the level BE decreases [10]. Unfortunately, such satellites are not well observed in the U4d XPS from $Cs_2UO_2Cl_4$,which is expected to exhibit a spin-orbit split doublet (ΔE_{sl}(U4d) = 42.5 eV). It is due to the relatively high $U4d_{3/2}$ FWHM ($\Gamma(U4d_{3/2})$ = = 4.7 eV) and the extra structure in all the U4d XPS BE range, as well as to the superposition with the $Cs3d_{3/2}$ XPS (fig. 3). It does not allow an accurate determination of the $U4d_{5/2}$ BE, FWHM and the shake-up satellite position. Since the spin-orbit splitting ΔE_{sl}(U4d) = 42.5 eV for UO_2F_2 [26] and $\Delta E_{sl}(U4d)_{theor}$ = 42.1 eV [41], the $U4d_{5/2}$ peak is expected at $E_b(U4d_{3/2})$ = 740.6 eV (fig. 3 and tab. 1). The $U4p_{3/2}$ peak was observed at $E_b(U4p_{3/2})$ = 1044.9 eV. The $U4p_{3/2}$ BE range XPS exhibits the complex structure that does not allow a correct determination of the FWHM and the shake-up parameters.

The multiplet splitting caused by the presence of the uncoupled Ln4f electrons in lanthanide compounds results in the Ln4d XPS structure [10]. Therefore, the multiplet splitting was expected to show up with the higher probability in the U5d XPS [6, 9]. Since the U(VI) ion does not contain the U5f electrons, the U5d XPS is not expected to exhibit the multiplet splitting. However, the U5d spectrum instead of a spin-orbit split doublet ($\Delta E_{sl}(U5d)_{theor}$ = 11.3 eV [41]) exhibits a complicated structure with the $U5d_{5/2}$ maximum at 98.1 eV (fig. 4). The U5d structure is superimposed with the Cs 4d satellite structure. The maxima of these satellites should be observed at ~87, ~99, and ~122 eV BE. However, these satellites are wide and contribute mostly to the spectral background. The U5d XPS consists of the two components with the shake-up

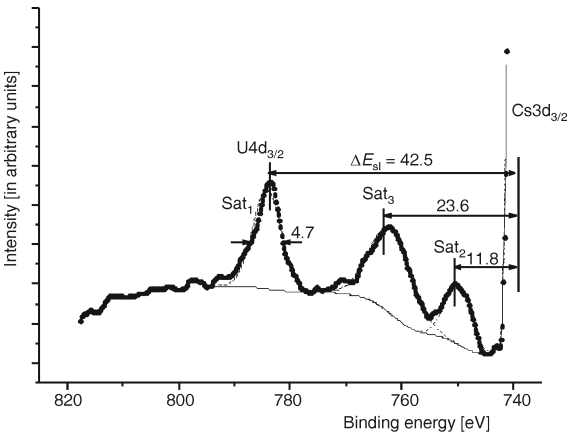

Figure 3. U4d XPS from $Cs_2UO_2Cl_4$

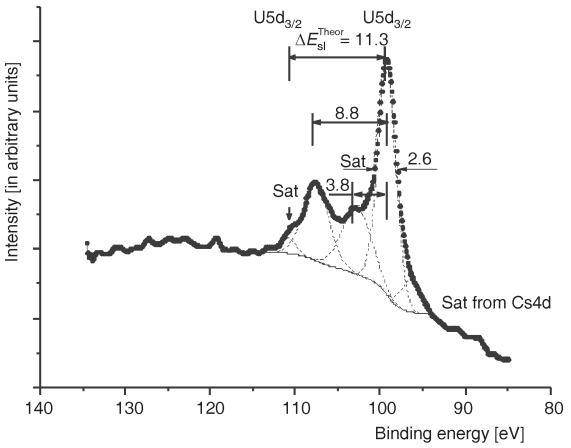

Figure 4. U5d XPS from $Cs_2UO_2Cl_4$; ΔE_{sl} is a theoretical value (tab. 1)

satellites at the higher BE side. Similar structure was observed in the U5d XPS from UO_2F_2 and γ-UO_3 [6]. The calculated $\Delta E_{sl}(U5d)_{theor.}$ = 11.3 eV is much higher than the corresponding values 8.8 and 8.7 eV for $Cs_2UO_2Cl_4$ and UO_2F_2 (tab. 1). For thorium compounds that do not contain the Th 5f electrons, the calculated $\Delta E_{sl}(Th5d)_{theor.}$= 7.08 eV [41] agrees satisfactorily with the experimental value 7.0 eV for ThO_2 and ThF_4 [6]. Special studies are required to understand the difference between the calculated and the experimental spin-orbit splitting E_{sl}(U5d).

Despite this, the $Cs_2UO_2Cl_4$ U5d XPS structure can be explained by the multiplet splitting superimposed with the shake-up satellites. Therefore, it is difficult to separate the satellite-related structure and to determine the satellite intensities. On moving from UO_2 to $Cs_2UO_2Cl_4$ the U5d XPS structure changes significantly. The distance between the most explicit peaks grows from 8.2 eV to 8.8 eV (tab. 1), and the shake-up satellites are observed at 3.8 eV instead of 6.9 eV [6] (fig. 4). On the basis of the above mentioned, one can conclude that the multiplet splitting does not complicate the valence XPS structure. This splitting must not show up in the U5s and the U6s XPS.

The dynamic effect related to the gigantic Coster-Kronig transitions, shows up in *e. g.* the U5p XPS of γ-UO_3 in the BE range ~190-270 eV [6]. The low intensity U5p XPS of $Cs_2UO_2Cl_4$ in this BE range is superimposed with the intense Cl2p (~199 eV BE), Cs4s (~230 eV BE) and Cl2s (~270 eV BE) peaks and their satellites. It does not allow one to separate the U5p-related components (tab. 1). With the data on the U5p XPS structure of γ-UO_3 [6], UO_2F_4, the Ba4p XPS [44], and the Ln 4p XPS of lanthanide oxides [10] in mind, one can attribute the U 5p XPS structure of $Cs_2UO_2Cl_4$ to the dynamic effect. It results in the U ion complex final state consisting of the ground one-hole state $U5p^55d^{10}5f^0$ and the excited two-hole state $U5p^65d^85f^1$. This suggestion is based on the U5p and the U5d BE ratio $E_b(U5p_{3/2})$ 200 eV and $E_b(PU5d_{5/2})$.= = 98.1 eV, which satisfies the condi-

tion: $E_b(U5p_{3/2})$ $2 \times E_b(U5d_{5/2})$. As a result, the probability of an extra-excited two-hole final state $U5p^6 5d^8 5f^1$ after the U5p photo emission, grows.

The U5s XPS of $Cs_2UO_2Cl_4$ is expected around E_b(U5s) ~323.7 eV [39,45]. However, the complex structure does not allow a reliable measurement of this spectrum. This structure can be attributed to the dynamic effect. The U6s XPS shows a widened (Γ(U6s) = 7.0 eV) structured line at 48.2 eV BE. One of the reasons for this U6s XPS structure can be suggested as the dynamic effect with the interaction of the configurations of the final states like $U6s^1 6p^6 d^0 5f^0$ and $U6s^2 6p^4 d^1 5f^0$. Indeed, for the E_b(U6s) = 48.2 eV, $E_b(U6p_{3/2})$ = 19.8 eV and $E_b(U6p_{1/2})$ = 30.9 eV, the condition E_b(U6s) $E_b(U6p_{3/2}) + E_b(U6p_{1/2})$ is satisfied, which does not contradict the possibility of the suggested configurations. The multiplet splitting- and the shake-up satellite-related structures are also possible in these spectra. This complicates the conclusion on the U6s electrons participation in the MO formation on the basis of the U6s XPS parameters.

As it was noted, multiplet splitting does not contribute much to the valence (0 - ~35 eV BE) XPS structure. The dynamic effect- related extra structure in this BE range is also low probable, since the atomic electronic states are absent in the valence BE range. As a result, the valence XPS structure can be associated with the MO formation, except for the spin-orbit split doublet at $E_b(Cs5p_{3/2})$ = 10.4 eV with ΔE_{sl}(Cs5p) = = 1.6 eV; and the Cs5s peak at E_b(Cs5s) = 23.8 eV (fig. 5). As it was noted, the extra structure in this BE range can also take place due to the electron energy loss appeared at the higher BE side from the Cs5p and Cs5s XPS peaks. Therefore, fig. 5(b), under the low BE $Cs_2UO_2Cl_4$ XPS gives the corresponding CsCl XPS normalized by the Cs5p intensity in order to show the Cs5p,5s contribution to the $Cs_2UO_2Cl_4$ XPS.

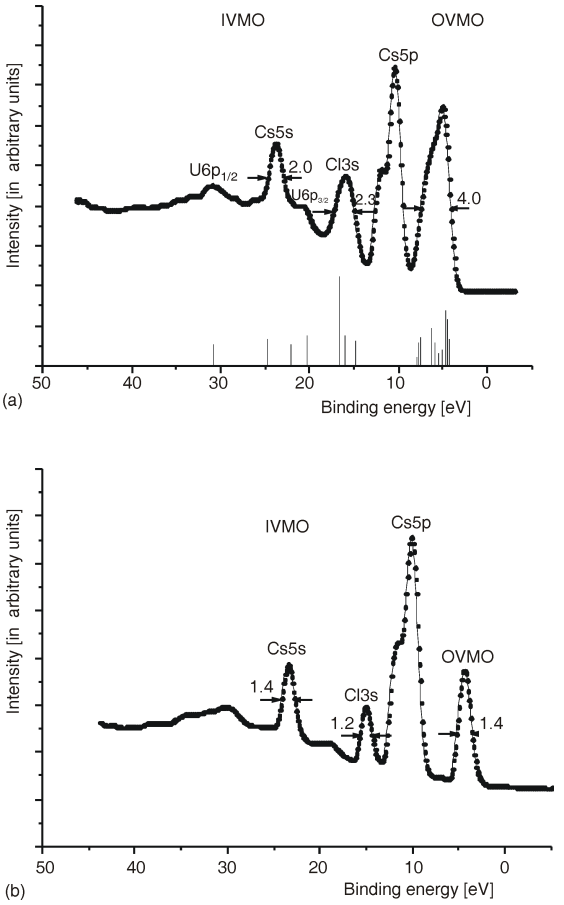

Figure 5. Valence band XPS: (a) – XPS from $Cs_2UO_2Cl_4$ with the secondarily scattered electrons background; the vertical bars show the calculated (RDV) spectrum; (b) – XPS from CsCl with the subtracted secondarily scattered electrons background; spectra normalized by the Cs5p intensity

Electronic structure of the $UO_2Cl_4^{2-}$ cluster

Electronic configuration of uranium ground state $^5L_6$ can be presented as $[Rn]6s^2 6p^6 5f^3 6d^1 7s^2 7p^0$, where [Rn] radon electronic configuration, and the other electronic shells are valence and can participate in the MO formation with the $O2s^2 2p^6$ and $Cl3s^2 3p^5$AOs in the $UO_2Cl_4^{2-}$ cluster. Results of the RDV electronic structure calculation of the $UO_2Cl_4^{2-}$ (D_{4h}) cluster reflecting U close environment structure in $Cs_2UO_2Cl_4$ are given in tab. 2. This calculation technique employed the MO LCAO (molecular orbitals as linear combinations of atomic orbitals) method, which allowed a discussion of the chemical bond nature in terms of atomic and molecular orbitals.

The chemical bond formation and the AO overlapping, result in the OVMO and the IVMO formation. Beside the U6s,6p,5f,6d,7s, O2s,2p, and Cl3s,3p AO, these MO include the U7p states, which are absent in atomic uranium. The RDV calculations show that the U6s AO, as well as the U7s and U7p AO, participate insignificantly in the MO formation (tab. 2). While the U5f AO participate mostly in the OVMO formation, the U6p,6d AO participate in formation of both the OVMO and the IVMO. The largest $U6p_{3/2,1/2}$ and the O2s AO mixing of the neighboring uranium and oxygen was observed for the $21\gamma_6^-$ (4) and $19\gamma_6^-$ (9) IVMO (tab. 2). The $U6p_{1/2}$ – O2s AO mixing in the $19\gamma_6^-$ (9) and the $18\gamma_6^-$ (10) IVMO is much higher than that in UO_2 because the interatomic distance $R_{U\text{-}O}$ in the uranyl group is lower than that in UO_2. A significant mixing was observed only for the $U6p_{3/2}$ and the Cl3s AO with formation of the $15\gamma_7^-$ (5) and the $14\gamma_7^-$ (7) IVMO. The obtained results suggest subdividing the valence MO into the three groups. The first group: $25\gamma_6^+$-$21\gamma_6^+$ OVMO. The second group: $21\gamma_6^-$ (4), $19\gamma_6^+$ (8), $19\gamma_6^-$ (9), $18\gamma_6^-$ (10) and $18\gamma_6^+$ IVMO characterizing the U-O binding in the axial direction. The third group: from $15\gamma_7^-$ (5), $20\gamma_6^-$, $15\gamma_7^+$, $20\gamma_6^+$ (6), $14\gamma_7^-$ (7) IVMO characterizing the U-Cl binding in the equatorial plane (tab. 2). These results allow one to understand the valence XPS structure of $Cs_2UO_2Cl_4$.

Table 2. MO composition (parts) and energies E_0[(a)] [eV] for the $UO_2Cl_4^{2-}$ cluster (RDV) and photo-ionization cross-sections σ_i[(b)]

MO		$-E_0$ [eV]	MO composition													
			Pu										O		Cl	
			6s	$6p_{1/2}$	$6p_{3/2}$	$6d_{3/2}$	$6d_{5/2}$	7s	$5f_{5/2}$	$5f_{7/2}$	$7p_{1/2}$	$7p_{3/2}$	2s	2p	3s	3p
			σ_i 1.14	0.89	1.29	0.61	0.55	0.12	3.67	3.48	0.07	0.10	0.96	0.07	1.26	0.47
OVMO	$28\gamma_6^+$	–16.14				0.28	0.49	0.08					0.07	0.06		0.02
	$31\gamma_6^-$	–9.56			0.01				0.03	0.03	0.87	0.01	0.01	0.02		0.02
	$22\gamma_7^+$	–9.18				0.06	0.72							0.04	0.02	0.15
	$30\gamma_6^-$	–8.91								0.01	0.01	0.95		0.01		0.02
	$21\gamma_7^+$	–8.80				0.32	0.46							0.13	0.02	0.07
	$24\gamma_7^-$	–8.78			0.01							0.96			0.02	0.01
	$27\gamma_6^+$	–8.66				0.42	0.32	0.03						0.18		0.06
	$26\gamma_6^+$	–8.05				0.06	0.01	0.78						0.02	0.02	0.11
	$29\gamma_6^-$	–7.45		0.01	0.07				0.12	0.34	0.06		0.02	0.37		0.01
	$20\gamma_7^+$	–5.72				0.41	0.42									0.17
	$23\gamma_7^-$	–4.29							0.10	0.64		0.01		0.22		0.03
	$28\gamma_6^-$	–3.95							0.43	0.28				0.21		0.08
	$27\gamma_6^-$	–3.03							0.03	0.84	0.01			0.02		0.10
	$22\gamma_7^-$	–2.77							0.06	0.85						0.09
	$21\gamma_7^-$	–2.22							0.76	0.09						0.15
	$20\gamma_7^-$	–1.95							0.79	0.17				0.01		0.03
	$25\gamma_6^{+(c)}$	0.00														1.00
	$26\gamma_6^-$	0.12			0.03				0.03	0.03		0.01		0.08		0.82
	$19\gamma_7^+$	0.26					0.01							0.07		0.92
	$24\gamma_6^+$	0.27				0.01								0.06		0.93
	$19\gamma_7^-$	0.43			0.01				0.03	0.02		0.01		0.02		0.91
	$18\gamma_7^-$	0.53			0.01				0.03	0.04				0.02		0.90
	$25\gamma_6^-$	0.57								0.08	0.01					0.91
	$17\gamma_7^-$	0.59							0.15	0.01		0.01				0.83
	$24\gamma_6^-$	0.85			0.01				0.03	0.04	0.02			0.02	0.01	0.87
	$18\gamma_7^+$	1.24				0.07	0.10									0.83
	$23\gamma_6^+$	1.60	0.01			0.01	0.01	0.05						0.11	0.02	0.79
	$17\gamma_7^+$	1.65				0.07	0.09								0.03	0.81
	$23\gamma_6^-$	2.06		0.01	0.07				0.11	0.27	0.01	0.02		0.34		0.17
	$16\gamma_7^-$	3.24			0.02				0.08	0.17				0.71		0.02
	$22\gamma_6^+$	3.28	0.01			0.01	0.04	0.03					0.06	0.78	0.01	0.06
	$22\gamma_6^-$	3.49		0.01					0.19	0.06				0.74		
	$16\gamma_7^+$	3.74				0.05	0.16							0.76		0.03
	$21\gamma_6^+$	3.84				0.05	0.07							0.75		0.03
IVMO	$21\gamma_6^-$	10.72		0.01	0.33				0.01	0.01		0.01	0.45	0.10	0.08	
	$15\gamma_7^-$	11.83			0.12							0.01		0.01	0.86	
	$20\gamma_6^-$	12.46		0.02	0.01					0.01	0.01		0.06		0.89	
	$15\gamma_7^+$	12.55				0.02	0.03								0.94	0.01
	$20\gamma_6^+$	12.64				0.01	0.01	0.03							0.94	0.01
	$14\gamma_7^-$	16.02			0.83									0.02	0.13	0.02
	$19\gamma_6^+$	17.95	0.02			0.05	0.06						0.85	0.02		
	$19\gamma_6^-$	20.50		0.25	0.41				0.01	0.01			0.27	0.03	0.01	0.01
	$18\gamma_6^-$	26.55		0.69	0.06				0.01				0.19	0.05		
	$18\gamma_6^+$	42.67	0.96										0.02	0.02		

[(a)] Levels shifted by 7.08 eV toward the positive values (upward); [(b)] photoionization cross-section $_i$ – kilo barn (10^{-25} m^2) per electron, for O and Cl from [42] and U from [43]; [(c)] HOMO (highest occupied MO) (two electrons), occupation number for all the orbitals is 2

Valence XPS structure of $Cs_2UO_2Cl_4$

The experimental valence band XPS of $Cs_2UO_2Cl_4$ exhibits a complicated structure, fig. 5(a). It can be suggested to consist of the XPS of the $UO_2Cl_4^{2-}$ ion and two Cs^+ ions. The valence XPS of the $UO_2Cl_4^{2-}$ cluster is superimposed with the $Cs5s^25p^66s^0$ XPS of two Cs^+ ions. Therefore, the CsCl XPS is given under the $Cs_2UO_2Cl_4$ XPS, fig. 5(b) for comparison. For comparison, the XPS spectra were normalized by the Cs5p intensity. The low BE CsCl XPS contains extra peaks at the higher BE side from the basic Cs5s and Cs5p peaks attributed to the shake-up satellites and other energy loss spectra.

These extra peaks complicate the interpretation of the $Cs_2UO_2Cl_4$ XPS. The contribution of this extra structure was taken into account on the analysis of the $Cs_2UO_2Cl_4$ and CsCl satellite structure in the 0-1250 eV BE range. It has to be taken into account that the XPS from Cs^+ ion in $Cs_2UO_2Cl_4$ can change compared to that from Cs^+ in CsCl. To evaluate this contribution, the difference spectrum was drawn. It was obtained by subtrac-

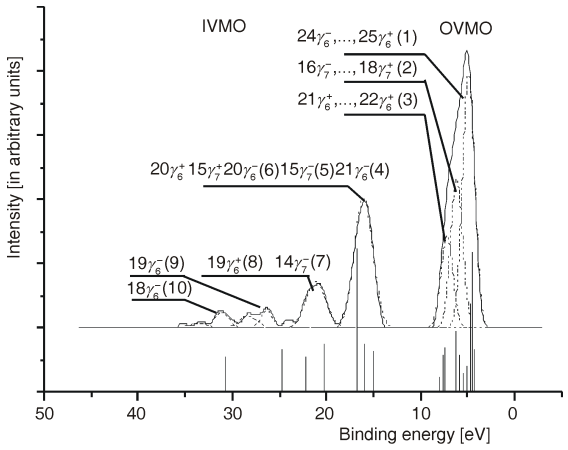

Figure 6. The difference of the valence XPS of $Cs_2UO_2Cl_4$ and 2 Cs^+ ions with the subtracted secondarily scattered electrons background (see fig. 5)

tion of the Cs^+ XPS, consisting of the Cs5s,5p peaks with satellites, from the $Cs_2UO_2Cl_4$ XPS, without taking into account the back scattering-related background (fig. 6). Despite the approximation inaccuracy, the resulting spectrum agrees qualitatively with the calculated spectrum for the $UO_2Cl_4^{2-}$ cluster.

To draw the difference spectrum, the XPS $Cs_2UO_2Cl_4$ and CsCl intensities were normalized to the Cs 5p intensity. It has to be noted, that on moving from CsCl to $Cs_2UO_2Cl_4$, the Cs5s and the Cs5p peaks shift to the higher BE region by 0.4 eV and 0.3 eV, respectively, and the Cl3s peak – shifts by 1.0 eV (tab. 1). The difference spectrum was drawn for the two cases: (a) without secondary scattered electrons-related background subtraction from the initial spectra; (b) with secondary scattered electrons-related background subtraction from the initial spectra (fig. 6). Despite the complicated structure, the difference spectra are in a satisfactory qualitative agreement.

The difference XPS characterizes the electronic structure of the $UO_2Cl_4^{2-}$ cluster and reflects its valence electrons structure (fig. 6). In the 0 -~35 eV BE range it can be conditionally subdivided into the two ranges. The first range 0 eV-~15 eV exhibits the OVMO-related structure. These OVMO are formed mostly from the U5f, 6d, 7s, 7p, the O2p and the Cl3p AO of the neighboring atoms. The second range ~15 eV-~35 eV exhibits the IVMO-related structure. These IVMO appear mostly due to the strong interaction of the completely filled U6p and O2s,Cl3s AO.

The OVMO XPS structure of the $UO_2Cl_4^{2-}$ cluster has its typical features and can be sub-divided into the three components (1-3) at 4.9, 6.1, and 7.2 eV BE, respectively (fig. 6, tab. 3). The peak at 4.9 eV BE is mostly due to the quasi-atomic U5f electrons of the $25\gamma_6^+$-$24\gamma_6^-$ OVMO participating in the chemical binding. The U5f electrons contribute significantly to the intensities of the bands at 6.1 eV and 7.2 eV. The fact that the calculated XPS OVMO (53.4 %) intensity is comparable with the corresponding experimental intensity (58.6 %),can be explained by the fact that the U5f electrons do not lose their *f*-nature participating in the chemical bond. It results in the widened XPS band in the OVMO BE range of $Cs_2UO_2Cl_4$, which agrees qualitatively with the calculation data (fig. 6, tab. 2).

The IVMO BE range exhibits explicit peaks and one can qualitatively pick out seven components (4-10; fig. 6). Despite the formalism of such a division, it allows qualitative and quantitative comparison of the XPS parameters with the relativistic calculation results for the $UO_2Cl_4^{2-}$ (D_{4h}) cluster.

Results of these calculations are given in tab. 2. Since photo emission results are given for an excited state of an atom with a hole in a certain shell, for a stricter comparison of the theoretical and experimental BE, the calculations must be done for transition states [46]. However, the valence electrons BE, calculated for transition states, are known to differ from the corresponding values for the ground state by a constant shift toward the higher energies. Therefore, the present paper gives the calculated BE (tab. 2) shifted by 4.17 eV (tab. 3). Taking into account the MO compositions (tab. 2) and the photo-ionization cross-sections [42, 43], the theoretical intensities of several XPS ranges were determined (tab. 3). Comparing the experimental XPS to the theoretical data, one should keep in mind that the $Cs_2UO_2Cl_4$ XPS reflects the band structure and consists of bands widened due to the solid-state effects. Despite this approximation, a satisfactory qualitative agreement between the theoretical and the experimental data was obtained (fig. 6).

The corresponding theoretical and experimental FWHM and the relative intensities of the inner and outer valence bands are comparable (tab. 3, fig. 6). A satisfactory agreement between the experimental and calculated BE of some MO was also reached (tab. 3). As previous noted, for the more accurate determination of the position of the $21\gamma_6^-$ OVMO (characterizing U-O bond) relative to the quasi-atomic $20\gamma_6^-$,$15\gamma_7^+$, $20\gamma_6^+$ (6) IVMO of chlorine, the calculations of $UO_2Cl_4^{2-}$ electronic structure at three interatomic distances around the equilibrium value: (a) $R_{U\text{-}O}$ = 0.171 nm and $R_{U\text{-}Cl}$ = 0.262 nm; (b) $R_{U\text{-}O}$ = = 0.174 nm, and $R_{U\text{-}Cl}$ = 0.264 nm; (c) $R_{U\text{-}O}$ = = 0.1772 nm and $R_{U\text{-}Cl}$ = 0.2671 nm, were done. On moving from (a) to (b) and (c), as it was expected, the outer and the inner valence bands narrow by 0.56 eV and 1.07 eV, respectively. The BE difference between the $15\gamma_7^-$ (5) and the $21\gamma_6^-$ (4) IVMO decreases by 0.29 eV, and the mean BE of the quasi-atomic chlorine-related IVMO $15\gamma_7^+$, $20\gamma_6^-$, $20\gamma_6^+$ (6) decreases by 0.12 eV. The alterations in the interatomic distances do not result in any significant changes of the XPS structure and position of the $21\gamma_6^-$ IVMO relative the quasi-atomic (6) IVMO of chlorine. These data prove the RDV method to be effective and allow the quantitative MO scheme for understanding the nature of interatomic bonding in $Cs_2UO_2Cl_4$.

Table 3. Valence XPS parameters for $Cs_2UO_2Cl_4$ and for the $UO_2Cl_4^{2-}$ cluster (RDV), and the orbital forces[(a)] f_O and f_{Cl}, U6p and U5f electronic state densities $\rho_i(e^-)$

MO		$-E$[(b)], [eV]	f_O, 10^{-8} N	f_{Cl}, 10^{-8} N	XPS			Am6p, 5f DOS ρ_i, e^- (electrons)			
					Energy[(c)] [eV]	Intensity [%]					
					Experiment	Theory	Experiment	$5f_{5/2}$	$5f_{7/2}$	$6p_{1/2}$	$6p_{3/2}$
OVMO	$25\gamma_6^{+(d)}$	4.17	–0.18	0.07		2.2		0.06	0.06		0.06
	$26\gamma_6^-$	4.29	–0.18	0.03		3.0					
	$19\gamma_7^+$	4.43	–0.13	0.08		2.1					
	$24\gamma_6^+$	4.44	–0.14	0.08		2.1					
	$19\gamma_7^-$	4.60	–0.18	0.08		4.7		0.06	0.04		0.02
	$18\gamma_7^-$	4.70	–0.18	0.07	4.9(1.5)	2.7	30.3	0.06	0.08		0.02
	$25\gamma_6^-$	4.74	–0.18	0.11		3.3			0.16		
	$17\gamma_7^-$	4.76	–0.19	0.10		4.5		0.30	0.02		
	$24\gamma_6^-$	5.02	–0.19	0.07		3.2		0.06	0.08		0.02
	$18\gamma_7^+$	5.41	–0.17	0.16		2.3					
	$23\gamma_6^+$	05.77	–0.19	0.09		2.0					
	$17\gamma_7^+$	5.82	–0.17	0.13		2.4					
	$23\gamma_6^-$	6.23	0.14	0.00	6.1(1.5)	7.2	17.7	0.22	0.54	0.02	0.14
	$16\gamma_7^-$	7.41	0.56	–0.03		4.5		0.16	0.34		0.04
	$22\gamma_6^+$	7.45	0.35	–0.02		0.9					
	$22\gamma_6^-$	7.66	0.62	–0.04	7.2(1.5)	4.5	10.9	0.38	0.12	0.02	
	$16\gamma_7^+$	7.91	0.60	–0.02		0.9					
	$21\gamma_6^+$	8.01	0.61	–0.01		0.9					
	Σf_i[(e)]		0.80	0.95		53.4	58.9	1.30	1.44	0.04	0.30
			(64.5 %)	(82.6 %)							
IVMO	$21\gamma_6^-$	14.89	–0.44	–0.05	14.9	4.8		0.02	0.02	0.02	0.66
	$15\gamma_7^-$	16.00	–0.12	0.01	16.0(2.3)	5.7	23.6				0.24
	$20\gamma_6^-$	16.63	–0.22	0.10		5.7			0.02	0.04	0.02
	$15\gamma_7^+$	16.72	–0.19	0.13	16.7	5.6					
	$20\gamma_6^+$	16.81	–0.18	0.14		5.6					
	$14\gamma_7^-$	20.19	–0.10	0.08	20.9(2.5)	5.7	10.2				1.66
	$19\gamma_6^+$	22.12	0.51	–0.05	22.0(2.5)	4.2					
	$19\gamma_6^-$	24.67	0.38	–0.02	26.3(2.2)	5.1	4.2	0.02	0.02	0.50	0.82
	$18\gamma_6^-$	30.72	0.78	–0.06	31.1(2.3)	4.2	3.1	0.02		1.38	0.12
	$\Sigma\rho_i$[(f)]					46.6	41.1	0.06	0.06	1.94	3.52
	$18\gamma_6^+$	46.67	0.02	–0.07	48.2(7.0)	4.9					
	Σf_2[(g)]		0.44	0.20							
			(35.5 %)	(17.4 %)							
	Σf[(h)]		1.24	1.15							

[(a)] Orbital force, newtons (N) per one ligand: f_O for U-O bond and f_{Cl} for Pu-Cl bondos; positive forces mean attraction, negative – repulsion
[(b)] Calculated energies (tab. 2) shifted by 4.17 eV toward the negative values (downward) so that the 15 γ_7^- MO energy is 16.0 eV
[(c)] FWHM in eV given in parentheses
[(d)] HOMO (highest occupied MO) (2 electrons), occupation number for all the orbitals is 2
[(e)] The sum of the OVMO orbital forces peak intensities and the U6p,5f DOS
[(f)] the sum of peak intensities and the U6p,5f DOS
[(g)] the sum of the IVMO orbital forces
[(h)] the sum of the OVMO and IVMO orbital forces

Thus, the outer valence band intensity is formed mostly from the outer valence U5f,6d,7s,7p and O2p,Cl3p AO, and to a lesser extent from the inner valence U6p and O2s, Cl3s AO. The U5f electrons contribute significantly to the OVMO intensity (tabs. 2 and 3). Because the U5f photo-emission cross-section is high (tab. 2), the U5f electrons contribute significantly to the OVMO XPS intensity if they do not lose the *f*-nature. Thus, the U5f electrons can be promoted to *e. g.* the U6d level first, and then to participate in the chemical bond formation losing the *f*-nature. The calculation shows that the U5f electrons participate directly in the formation of the chemical bond (tab. 2). The calculated OVMO/IVMO intensity ratio for the $UO_2Cl_4^{2-}$ XPS was found to be 1.15, which differs from the experimental value 1.43 (tab. 3) due to the error in the XPS difference spectrum. This intensity ratio is an important quantitative characteristic of the $UO_2Cl_4^{2-}$ electronic structure. These results yield a conclusion that the U5f electrons can participate directly in the chemical bond formation in $UO_2Cl_4^{2-}$ partially losing the *f*-nature. These electronic states are distributed within the outer valence band (tab. 2). It agrees with the OVMO XPS shape. The U6d electronic states are located mostly at the bottom of the outer valence band. The $U6p_{3/2}$ AO take a significant part in the OVMO formation. This agrees with the theoretical and the experimental data for γ-UO_3 [14] and UF_2O_2 [26].

In the IVMO XPS BE range a satisfactory agreement was reached *e. g.* for the $21\gamma_6^-$ (4) and $18\gamma_6^-$ (10) MO responsible for the width ΔE of this XPS band. The

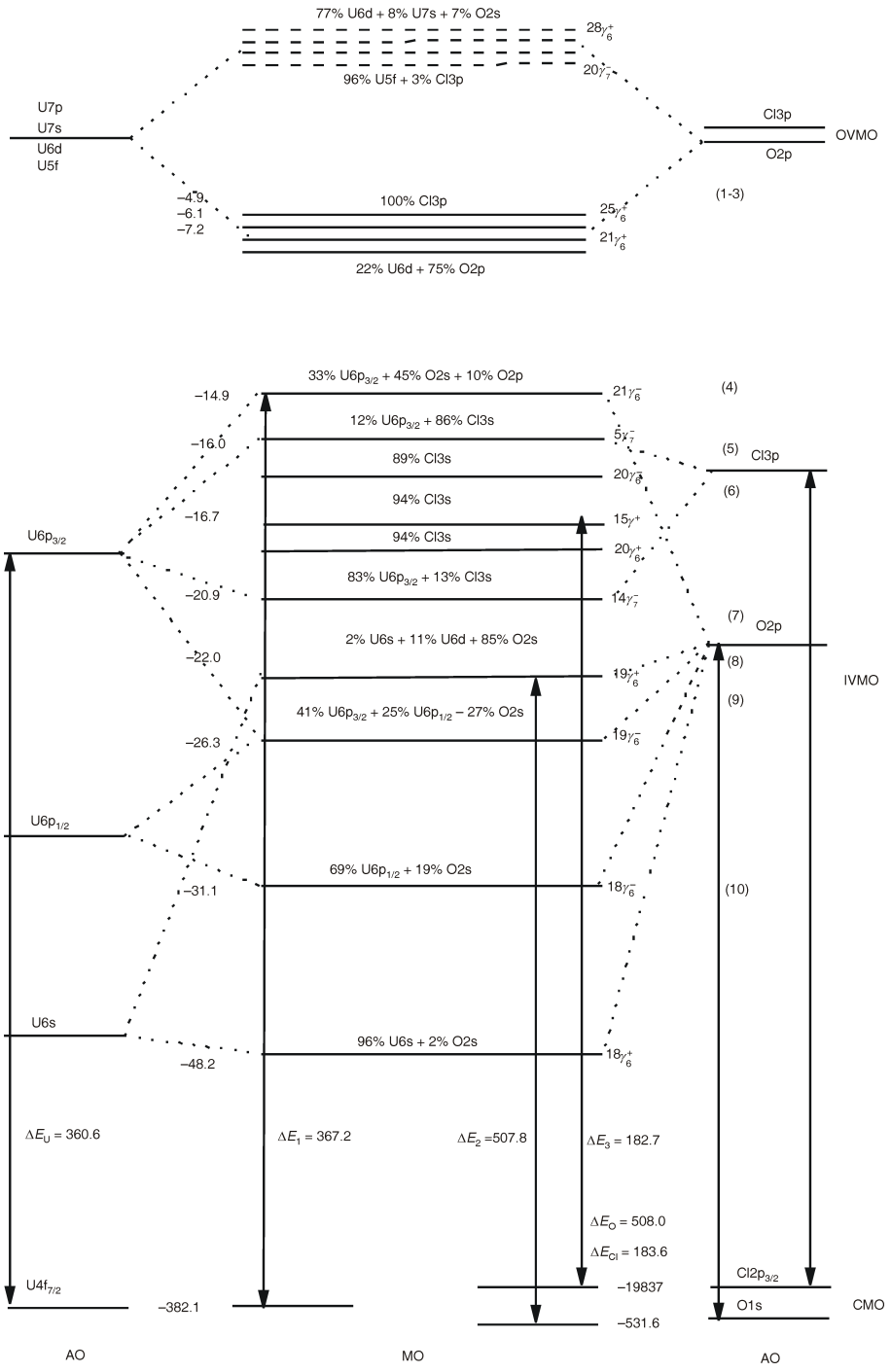

Figure 7. MO scheme for the $UO_2Cl_4^{2-}$ (D_{4h}) cluster built taking into account theoretical and experimental data; chemical shifts are not indicated; arrows show some measurable levels BE differences; experimental BE [eV] are given to the left; the energy scale is not kept

calculated ΔE_{theor} = 15.83 eV agrees with the experimental ΔE_{exp} = 16.2 eV without taking into account the FWHM (tab. 3). It has to be noted that the theoretical (1.15) and experimental (1.4) OVMO/IVMO intensity ratios are comparable. It confirms correctness of the approximations used in the calculation (tab. 3). The calculated and the experimental relative intensities of some individual IVMO peaks, except for the $14\gamma_7^-$ (7), $19\gamma_6^+$ (8) ones, are in a qualitative agreement.

Taking into account the experimental BE differences between the outer MO and the core levels in the $UO_2Cl_4^{2-}$ cluster and metallic U [39, 40], as well as the relativistic MO LCAO calculation data for the $UO_2Cl_4^{2-}$ (D_{4h}) cluster, a quantitative MO scheme for this cluster was built (fig. 7). This scheme allows one to understand the real XPS structure and the chemical bond nature in the $UO_2Cl_4^{2-}$ cluster. In this approximation, one can pick out the anti bonding $21\gamma_6^-$ (4) and $15\gamma_7^-$ (5) and the corresponding bonding $19\gamma_6^-$ (9) and $14\gamma_7^-$ (7) IVMO, as well as the quasi-atomic $20\gamma_6^-$, $15\gamma_7^+$, $20\gamma_6^+$ (6) ones attributed mostly to the Cl3s and the $19\gamma_6^+$ (8) attributed mostly to the O2s electrons and

the $18\gamma_6^+$ one.The experimental data show that the Cl3s- related quasi-atomic IVMO BE have to be close by an order of magnitude.

Indeed, the Cl3s XPS peak of CsCl (Eb(Cl3s) = = 15.0 eV) is 1.2 eV wide. In $Cs_2UO_2Cl_4$ XPS this peak is observed at E_b(Cl3s) = 16.0 eV and is 2.3 eV wide (tab. 1). The BE shift and widening is associated with the Cl3s AO participation in the IVMO formation (fig. 7).

The Cs5p XPS was observed as a spin-orbit split doublet in the band-gap between the OVMO and IVMO at $E_b(Cs5p_{3/2})$ = 10.4 eV and ΔE_{sl}(Cs5p) = = 1.6 eV, fig. 5(a).

The Cs 5s peak in the $Cs_2UO_2Cl_4$ XPS was observed single at E_b(Cs5s) = 23.8 eV and Γ(Cs5s) = = 2.0 eV. It was superimposed with the O2s peak attributed to the uranyl group UO_2^{2+}. It has to be noted that cesium peaks were observed intense in the whole BE range 10-1250 eV. The Cs XPS of CsCl exhibits an extra structure at the higher BE side from the basic peaks E_{sat1} = 9.4 eV and E_{sat2} = 23.4 eV. It can be attributed to the electron energy loss processes during photo emission. Such a structure was observed in the core chlorine XPS of CsCl at ΔE_{sat3} = 19.3 eV, see *e. g.* fig. 5(b). This structure complicates the interpretation of the valence $Cs_2UO_2Cl_4$ XPS.

The O1s peak was observed symmetric and 1.6 eV wide (fig. 1), while the BE of the quasi-atomic $19\gamma_6^+$ (8) IVMO should be about 23.6 eV since E_O = 508.0 eV and the O1s BE in $Cs_2UO_2Cl_4$ XPS is E_b(O1s) = = 531.6 eV (tab. 1).

The experimental E_U = 360.6 eV [39, 40] is comparable with the calculated value 361.0 eV [41], and the difference E_1 = 367.2 eV, one can find that $_1 = E_1 - E_U$ is 6.6 eV (fig. 7). Since the BE difference between the $21\gamma_6^-$ (4) and $18\gamma_6^-$ (10) IVMO is 16.2 eV, and the U6p spin-orbit splitting, according to the calculation data [41], is E^t_{sl}(U6p) = 10.0 eV and that according to the experimental data – 10.0 eV [39, 40], one can evaluate that the perturbation $_1$ = 6.2 eV agrees satisfactorily with the corresponding value of 6.6 eV, found from the BE difference between the core and the valence MO. The observed difference (0.4 eV) must be attributed to the IVMO formation peculiarities and such a comparison may not be quite correct. However, these data show that the $21\gamma_6^-$ (4) IVMO has a significant anti bonding nature.The IVMO FWHM cannot yield a conclusion on the IVMO nature (bonding or anti bonding), however, one can suggest that the admixture of 10 % of the O2p and 2 % of the U5f AO in the $21\gamma_6^-$ (4) IVMO leads this orbital to loosing of itsanti-bonding nature (tab. 2, fig. 7, see also [6]). Thus, the quantitative MO scheme for $UO_2Cl_4^{2-}$, built on the basis of the experimental and the theoretical data, allows one both to understand the nature of chemical bond formation in $Cs_2UO_2Cl_4$ and to interpret the structures of other X-ray spectra as it was shown for γ-UO_3 [14] and UO_2F_2 [26].

Chemical bond in the $UO_2Cl_4^{2-}$ cluster

As it was noted, the calculation data show that the MO system of the $UO_2Cl_4^{2-}$ cluster can be subdivided into several groups (tab. 2, fig. 7). One group associated with the UO_2^{2+} ion includes the $18\gamma_6^+$, $18\gamma_6^-$ (10), $19\gamma_6^-$ (9), $19\gamma_6^+$ (8), and $21\gamma_6$ (4) IVMO characterizing the U-O bond in the axial direction. Another group from the $14\gamma_7^-$ (7) to the $15\gamma_7^-$ (5) IVMO consists of the Cl3s and U6p AO. Another one – from the $21\gamma_6^+$ to the $25\gamma_6^+$ OVMO represents the valence band. In the lower part of this band there are the O 2p-type bonding MO with the admixtures of U valence states, the middle and the upper parts – consist of the Cl3p MO with admixtures of metal MO (tab. 2).

By the present time there is no method to evaluate quantitatively a contribution of certain separate MO into the chemical bond even for diatomic molecules. Such a method has to be additive, *i. e*. the summation of contributions of separate MO with electron populations in mind has to yield the total chemical bond value. The work [5] considers three methods of evaluation of the MO nature (bonding, non-bonding, anti bonding) on the basis of: (a) population by Mulliken, (b) full energy separation with subtraction of resonance energy characterizing the covalence of the chemical bond, and (c) orbital forces.

The orbital forces f_i (10^{-8} N) are equal approximately to the derivatives of the MO energies E_i' (10^{-8} N) upon the interatomic distances [5]. Therefore, this work presents the dependence of the MO energies for the $UO_2Cl_4^{2-}$ cluster on the interatomic distance in the axial direction $R_{U\text{-}O}$ (Z-axis) and in the equatorial plane $R_{U\text{-}Cl}$. To evaluate the orbital forces in addition to the calculation for the equilibrium atomic positions ($R_{U\text{-}O}$ = = 0.1772 nm, $R_{U\text{-}Cl}$ = 0.2671 nm), two more calculations were also done. One for $R_{U\text{-}O}$ = 0.1792 nm and the invariable positions of chlorine ions, and another one – with equal positions of oxygen ions but with increased U-Cl distance to the four chlorine ions $R_{U\text{-}Cl}$ = 0.2691 nm. It yielded the orbital forces f_i (derivatives E_i' of the OVMO and IVMO energies E_i upon the interatomic distances $R_{U\text{-}O}$ and $R_{U\text{-}Cl)}$ (tab. 3).

As it follows from tab. 3 and the MO scheme (fig. 7), the $18\gamma_6^+$,$18\gamma_6^-$ (10), $19\gamma_6^-$ (9), $19\gamma_6^+$ (8) IVMO from this group, bring a significant bonding contribution (1.69 10^{-8} N) to the U-O binding and a slight anti-bonding contribution (–0.20 10^{-8} N) to the U-Cl interaction. On the other hand, the IVMO of the other group from the $14\gamma_7^-$ (7) to the $15\gamma_7^-$ (5) containing the Cl3s states, bring a significant bonding contribution (0.46 10^{-8} N) to the U-Cl interaction and an anti-bonding contribution (–0.81 10^{-8} N) to the U-O binding. As it was expected, the bonding OVMO around the valence band bottom ($21\gamma_6^+$-$23\gamma_6^-$) contribute significantly (2.88 10^{-8} N) to the U-O binding, even despite the anti-bonding nature (–2.08 10^{-8} N) of the other OVMO of this group. The total OVMO con-

tribution to the U-O bond is 0.80 10^{-8} N. The total OVMO contribution to the U-Cl binding per one bond is 0.95 10^{-8} N, which is comparable to that for the U-O bond. On the basis of these data the relative IVMO contribution to the U-O binding per one bond in the $UO_2Cl_4^{2-}$ cluster was evaluated as 33.5 %, and that of the OVMO contribution – 64.5%. The relative IVMO contribution to the U-Cl binding is 17.4 %, that of the OVMO – 82.6% (tab. 3).

The structures of irreducible representations of the double D_{4h} group allows comparisons of the U6d and the U5f AO participation in the chemical bond since the γ_6^+ and γ_7^+ orbitals contain the 6d states and do not contain the 5f states, while the $_6^-$ and the $_7^-$ MO – *vice versa*, contain the 5f states and do not contain the 6d states. Table 3 shows that among the six bonding MO in the lower part of the OVMO band there are three orbitals of each type. The fractions of the 6d AO in the $21\gamma_6^+$, $16\gamma_7^+$ and $22\gamma_6^+$ MO are 0.22, 0.21, and 0.05, respectively, while the fractions of the 5f AO in the $22\gamma_6^-$, $16\gamma_7^-$ and $23\gamma_6^-$ MO are 0.25, 0.25, and 0.38, respectively (tab. 2). Despite the fact that the fraction of the 5f AO is greater than that of the 6d AO, their contributions are comparable, and the last $23\gamma_6^-$ orbital shows the least orbital force (0.14 10^{-8} N) among the six considered bonding MO. Among the U-Cl bond-related OVMO, the upper MO starting with the $17\gamma_7^+$ show the highest orbital forces. The bonding role of the 6d states in the U-Cl binding is also slightly higher than that of the 5f states. These results agree with the values of the overlapping populations for the corresponding orbitals, found in the present work. These results also agree with the data on the covalent contribution of the uranyl group UO_2^{2+} with $R_{U\text{-}O} = 0.173$ nm to the IVMO. For the uranyl group the method of the full energy separation and X -DV determination of the resonance energy E^R(eV) showed that the IVMO electrons contribution to the covalent component of the chemical bond is 37 % of the total contribution of all the MO [5]. It agrees with the fact that the IVMO electrons play a significant role in the chemical bond in $Cs_2UO_2Cl_4$. The obtained data agree qualitatively with those for $Cs_2PuO_2Cl_4$ [47].

CONCLUSIONS

With the core electron XPS structure, BE differences between the core and the valence electronic levels and the relativistic calculation results of the electronic structure of the $UO_2Cl_4^{2-}$ (D_{4h}) cluster in mind, a quantitative interpretation of the valence XPS structure in the BE range 0 eV to ~35 eV for $Cs_2UO_2Cl_4$, was done. The correlation of the XPS structure parameters with the mechanisms of its formation was established.

The U5f (2.86 U5f e^-) electrons, delocalized within the outer valence band, were theoretically shown and experimentally confirmed to participate directly in the chemical bond formation in $Cs_2UO_2Cl_4$ partially losing their *f*-nature.

The U6p electrons, in addition to the effective (experimentally measurable) participation in the IVMO formation, were found to participate noticeably (0.34 U6p e^-) in the filled OVMO formation.

The largest part in the IVMO formation in $Cs_2UO_2Cl_4$ was established to be taken by the $U6p_{1/2,3/2}$ and the O2s AO, and to a lesser extent – by the $U6p_{3/2}$ and the Cl3s AO, of the neighboring uranium oxygen and chlorine ions.

The MO sequent order in the BE range of 0 eV to ~35 eV for the $UO_2Cl_4^{2-}$ cluster was defined and the corresponding MO composition was obtained. This yielded a fundamental quantitative MO scheme, which is important for understanding the nature of interatomic bonding in $UO_2Cl_4^{2-}$ and for the interpretation of other X-ray spectra of $Cs_2UO_2Cl_4$.

The OVMO and IVMO contributions to the chemical bond were evaluated for the $UO_2Cl_4^{2-}$ cluster. The relative OVMO contribution to the chemical binding was shown to be 76 %, and that of the IVMO – 24 %. Despite the approximations used for the evaluation of the IVMO and OVMO contributions were not perfect, one can conclude that the theoretical and experimental studies of chemical bond cannot neglect the IVMO formation effect in actinide compounds.

ACKOWLEDGEMENTS

The work was supported by the RFBR grant no. 13-03-00214-a.

AUTHORS' CONTRIBUTIONS

The idea for the study was put forward by Yu. A. Teterin, the measurements were carried out by K. I. Maslakov, the theoretical calculations were carried out by M. V. Ryzhkov, the compounds were produced by D. N. Suglobov, the samples were prepared by V. G. Petrov, experimental data were processed and interpreted by A. Yu. Teterin, K. E. Ivanov, and S. N. Kalmykov.

REFERENCES

[1] Veal, B. W., *et al*., X-Ray Photoelectron Spectroscopy Study of Hexavalent Uranium Compounds, *Phys. Rev. B., 12* (1975), pp. 5651-5663

[2] Verbist, J., *et al*., X-Ray Photoelectron Spectra of Uranium and Uranium Oxides, Correlation with the Half-Life of $^{235}U^m$, *J. Electr. Spectr. Relat. Phenom., 5* (1974), pp. 193-205

[3] Teterin, Yu. A., *et al*., The XPS Structure of the Low-Energy Electrons of Oxides UO_2 and γ-UO_3, (in Russian), Doklady Akademii Nauk SSSR, *(Reports of the Academy of Sciences of USSR), 256* (1981), 2, pp. 381-384

[4] Thibaut, E., *et al*., Electronic Structure of Uranium Halides and Oxyhalides in the Solid State, an X-Ray

Photoelectron Spectroscopy Study of Bonding Iconicity, *J. Am. Chem. Soc., 104* (1982), pp. 266-5273
[5] Teterin, Yu. A., Gagarin, S. G., Inner Valence Molecular Orbitals and the Structure of X-Ray Photoelectron Spectra, *Russian Chemical Reviews, 65* (1996), 10, pp. 825-847
[6] Teterin, Yu. A., Teterin, A. Yu., Structure of X-Ray Photoelectron Spectra of Light Actinide Compounds, *Russian Chemical Reviews, 73* (2004), 6, pp. 541-580
[7] Veal, B.W., Lam, D. J., Diamond, H., X-Ray Photoelectron Spectroscopy of 5f Electrons in Dioxides of Neptunium and Plutonium, *Physica B, 86-88* (1977), pp. 1193-1194
[8] Tobin, J. G., Yu, S.-W., Orbital Specificity in the Unoccupied States of UO_2 from Resonant Inverse Photoelectron Spectroscopy, *Phys. Rev. Letters., 107* (2011), 167406
[9] Beatham, N., Orchard, A. F., Thornton, G., On the Photoelectron Spectra of UO_2, *J. Electron Spectrosc. Relat. Phenom., 19* (1980), pp. 205-211
[10] Teterin, Yu. A., Teterin, A. Yu., Structure of X-Ray Photoelectron Spectra of Lanthanide Compounds, *Russian Chemical Reviews, 71* (2002), 5, pp. 347-381
[11] Ellis, D. E., Rosen, A., Walch, P. F., Applications of the Dirac-Slater Model to Molecules, *Intern. J. Quant. Chemist. Symp., 9* (1975), pp. 351-358
[12] Walch, P. F., Ellis, D. E., Effects of Secondary Ligands on the Electronic Structure of Uranyls, *J. Chem. Phys., 65* (1976), 6, pp. 2387-2392
[13] Hirata, M., *et al*., Valence Electronic Structure of Uranyl Nitrate $UO_2(NO_3)_2$ $2H_2O$, *J. Electr. Spectr. Relat. Phenom., 83* (1997), pp. 59-64
[14] Teterin, Yu. A., *et al*., The Nature of Chemical Bond in Trioxide γ-UO_3, *Nucl Technol Radiat, 17* (2002), 1-2, pp. 3-12
[15] Boring, M., Wood, J. H., Miscowitz, J. M., Self-Consistent Field Calculation of the Electronic Structure of the Uranyl Ion (UO_2^{++}), *J. Chem. Phys., 63* (1975), 2, pp. 638-642
[16] Denning, R. G., Electronic Structure and Bonding in Actinyl Ions., *Structure and Bonding, 79* (1992), pp. 215-276
[17] Denning, R. G., Electronic Structure and Bonding in Actinyl Ions and their Analogs, *J. Chem. Phys., A 111* (2007), pp. 4125-4143
[18] Atuchin, V. V., Zhang, Z., Chemical Bonding Between Uranium and Oxygen in U^{6+}-Containing Compounds, *J. Nucl. Mater., 420* (2012), pp. 222-225
[19] Wadt, W. R., Why UO_2^{2+} is Linear and Iso Electronic ThO_2 is Bent, *J. Am. Chem. Soc., 103* (1981), pp. 6053-6057
[20] Tatsumi, K., Hoffmann, R., Bent cis d^0 MoO_2^{2+} *vs* Linear Trans d^0f^0 UO_2^{2+}: A Significant Role for Non Valence 6p Orbital in Uranyl, *Inorg. Chem., 19* (1980), pp. 2656-2658
[21] Teterin, Yu. A., *et al*., The Role of the Low-Energy Filled Sub-Shells Electrons in the Chemical Bond of Uranium Compounds (in Russian), *Doklady Akademii Nauk SSSR (Reports of the Academy of Sciences of USSR) 284* (1985) 4, pp. 915-920
[22] de Jong, W. A., Visscher, L., Nieupoort, W. C., On the Bonding and the Electric Field Gradient of the Uranyl Ion, *J. Molecular Structure (Theochem), 458* (1999), pp. 41-52
[23] Ilton, E. S., Bagus, P. S., XPS Determination of Uranium Oxidation States, *Surf. Interface Anal., 43* (2011), pp. 1549-1560
[24] Pireaux, J. J., *et al*., The Potential Use of Uranium Oxides and Uranium-Bismuth Mixed Oxides in Catalysis, *Chem. Phys., 22* (1977), pp. 113-120
[25] Teterin, Yu. A., Teterin, A. Yu., Modern X-Ray Spectral Methods in the Study of the Electronic Structure of Actinide Compounds: Uranium Oxide UO_2 as an Example, *Nucl Technol Radiat, 19* (2004), 2, pp. 3-14
[26] Utkin, I. O., *et al.*, X-Ray Spectral Studies of the Electronic Structure of Uranyl Fluorite UO_2F_2, *Nucl Technol Radiat, 19* (2004), 2, pp. 15-23
[27] Teterin, Yu. A., *et al.*, Nature of the Chemical Bond in Uranium Dioxide UO_2, *Radiochemistry, 47* (2005), 3, pp. 215-224
[28] Hall, D., Rae, A. D., Waters, T. N., The Crystal Structure of Dicasiumtetrachlorodioxourannium (VI), *Acta Cryst., 2* (1966), pp. 160-162
[29] Shirley, D. A., High-Resolution X-Ray Photoemission Spectrum of the Valence Band of Gold, *Phys. Rev. B., 5* (1972), pp. 4709-4714
[30] Teterin, Yu. A., *et al*., Correlation of the XPS Structure of Plutonium and Uranium in $Cs_2AnO_2Cl_4$ (An = Pu,U) Single Crystals with Their Oxidation States, Structure and Chemical Bond Nature, (in Russian), *Doklady Akademii Nauk SSSR (Reports of the Academy of Sciences of USSR), 277* (1984), 1, pp. 131-136
[31] Gouder, T., Havela, L., Examples of Quantification in XPS on 5f Materials, *Mikrochim. Acta., 138* (2002), pp. 207-215
[32] Watkin, D. J., Denning, R. G., Prout, K., Structure of dicaesiumtetrachlorodioxouranium (VI), *Acta Crystallogr., C47* (1991), pp. 2517-2519
[33] Wilkerson, M. P., Scott, B. L., Dicaesiumtetrachloridodioxidoplutonat (VI), *Acta Cryst., E64* (2008), i5, sup-1- sup-6
[34] Rosen, A., Ellis, D. E., Relativistic Molecular Calculations in the Dirac-Slater Model, *J. Chem. Phys., 62* (1975), 8, pp. 3039-3049
[35] Adachi, H., Relativistic Molecular Orbital Theory in the Dirac-Slater Model, *Technical Report Osaka University, 1392* (1977), 27, pp. 569-576
[36] Gunnarsson, O., Lundqvist, B. I., Exchange and Correlation in Atoms, Molecules, and Solids by the Spin-Density-Functional Formalism, *Phys. Rev. B., 13* (1976), 10, pp. 4274-4298
[37] Pyykko, P., Toivonen, H., Tables of Representation and Rotation Matrices for the Relativistic Irreducible Representations of 38 Point Groups, *Acta Acad. Aboensis, Ser. B, 43* (1983), pp. 1-50
[38] Varshalovish, D. A., Moskalev, A. N., Khersonskii, V. K., Quantum Theory of Angular Momentum World Scientific, Singapore 1988, p. 439
[39] Fuggle, J. C., *et al*., X-Ray Photoelectron Studies of Thorium and Uranium, *J. Phys. F: Metal Phys., 4* (1974), pp. 335-342
[40] Fuggle, J. C., Martensson, N., Core-Level Binding Energies in Metals, *J. Electron Spectrosc. Relat. Phenom., 21* (1980), pp. 275-281
[41] Huang, K. N., *et al*., Neutral-Atom Electron Binding Energy from Relaxed-Orbital Relativistic Hartree-Fock-Slater Calculations, *At. Data Nucl. Data Tables, 18* (1976), pp. 243-291
[42] Band, M., Kharitonov, Y. I., Trzhaskovskaya, M. B., Photoionization Cross Sections and Photoelectron Angular Distribution for X-Ray Line Energies in the range 0.132-4.509 keV (Targets: 100 Z 1), *At. Data Nucl. Data Tables, 23* (1979), pp. 443-505
[43] Yarzhemsky, V. G., et al., Photoionization Cross-Sections of Ground and Excited Valence Levels of actinides, *Nucl Technol Radiat, 27* (2012), 2, pp. 103-106
[44] Yarzhemsky, V. G., Teterin, Y. A., Sosulnikov, M. I., Dynamic Dipolar Relaxation in X-Ray Photoelectron Spectra of Ba4p Subshell in Barium Compounds, *J. Electron Spectrosc. Relat. Phenom., 59* (1992), pp. 211-222

[45] Sevier, K. D., Atomic Electron Binding Energy, *Atomic Data and Nuclear Data Tables, 24* (1979), pp. 323-371
[46] Slater, J. C., Johnson, K. H., Self-Consist Field X Cluster Method for Poly Atomic Molecules and Solids, *Phys. Rev. B, 5* (1972), pp. 844-853
[47] Teterin, Yu. A., *et al*., Electronic Structure and Chemical Bond Nature in $Cs_2PuO_2Cl_4$, *Nucl Technol Radiat, 30* (2015), 2, pp. 99-112

Received on February 25, 2016
Accepted on March 7, 2016

Јурий А. ТЕТЕРИН, Константин И. МАСЛАКОВ, Михаил В. РИШКОВ, Антон Ј. ТЕТЕРИН, Кирил Е. ИВАНОВ, Степан Н. КАЛМИКОВ, Владимир Г. ПЕТРОВ, Дмитриј Н. СУГЛОБОВ

ВАЛЕНТНА СТРУКТУРА РЕНДГЕНСКИХ ФОТОЕЛЕКТРОНСКИХ СПЕКТАРА И ХЕМИЈСКА ВЕЗА У $Cs_2UO_2Cl_4$

Обављена је квантитативна анализа структуре рендгенских фотоелектронских спектара валентних електрона у области енергија везе од 0 eV до ~35 eV у кристалном дицезијум тетрахлоридоксоуранијуму ($Cs_2UO_2Cl_4$), једињењу које садржи уранил групу UO_2^{2+}. При томе су урачунате енергије везе и структуре електронских љуски језгра (~35 eV-1250 eV), као и резултати релативистичког дискретног варијационог прорачуна $UO_2Cl_4^{2-}(D_{4h})$ кластера који одражава блиску околину уранијума у $Cs_2UO_2Cl_4$. Експериментални подаци показују да ефекти више тела услед присуства цезијума и хлора доприносе спољашњој валентној спектралној структури (енергије везе 0-~15 eV) много мање него унутрашњој (енергије везе ~15-~35 eV ВЕ). Теоретски је прорачунато и експериментално потврђено да су унета U5f електронска стања присутна у валентној зони $Cs_2UO_2Cl_4$. То поткрепљује претпоставку о непосредном уделу U5f електрона у хемијској вези. Електрони U6p атомских орбита учествују у настанку и унутрашњих и спољашњих валентних молекулских орбита (зона). Установљено је да U6p, O2s и Cl3s електронске љуске највише доприносе настанку унутрашњих валентних молекулских орбита. Одређени су композиција и секвенцијални поредак молекулских орбита у области енергија везе од 0 eV до ~35 eV за $UO_2Cl_4^{2-}$ кластер. Експериментални и теоретски подаци допуштају да се квантификује шема молекулских орбита за UO_2Cl_{42} кластер у области енергија везе од 0 eV до ~35 eV, што је битно и за разумевање природе хемијске везе и тумачењу других рендгенских спектара $Cs_2UO_2Cl_4$. Процењено је да допринос спољашњих валентних молекулских орбита хемијском везивању $UO_2Cl_4^{2-}$ кластера износи 76 %, док је допринос унутрашњих орбита 24 %.

Кључне речи: актинид, уранијум, електронска структура, рендгенска фотоелектронска спектроскопија, релативистички прорачун